

Ultraviolet Resonance Raman Studies of Trans and Cis Peptides: Photochemical Consequences of the Twisted π^* Excited State

Sunho Song,[†] Sanford A. Asher,^{*,†} Samuel Krimm,[‡] and Keith D. Shaw[‡]

Contribution from the Department of Chemistry, University of Pittsburgh, Pittsburgh, Pennsylvania 15260, and the Biophysics Research Division, University of Michigan, Ann Arbor, Michigan 48109. Received February 22, 1990

Abstract: Excitation into the amide $\pi-\pi^*$ transitions of *N*-methylacetamide (NMA) and small peptides such as di- and triglycine results in the photochemical conversion of the *trans*-amides into *cis*-amides with a high quantum yield. The *cis* form of NMA is easily monitored since its amide II UV Raman cross section is ca. 10-fold larger than that of the *trans* peptide with 220-nm excitation. We can detect the ca. 1.5% Boltzmann population of the *cis* form of NMA present at room temperature. The amide II mode of *cis* peptides differs dramatically from that of *trans* peptides since it contains much less N-H in-plane bending. This result is inconsistent with previous normal mode calculations which assumed identical geometry and force constants for the *cis* and *trans* forms. The π^* excited state of peptides is twisted relative to the ground state in a manner reminiscent of ethylene. We also reinterpret previous studies of *N*-methylthioacetamide to indicate that its π^* excited state is twisted. Our data clearly indicate the correctness of the assignment of the peptide conformation sensitive band at ca. 1400 cm^{-1} to the overtone of the amide V vibration for dipeptides and polypeptides. The fact that the overtone of the amide V vibration is not enhanced for NMA and related derivatives indicates a significant difference between the NMA excited-state potential surface and that of dipeptides and polypeptides. This result may signal that the peptide π^* excited state is delocalized over the peptide backbone.

Introduction

The specific conformation of a protein determines its reactivity and dynamics.¹⁻³ This macromolecular ordering, which is in large part determined by the protein primary structure and by inter-residue interactions, specifies the three-dimensional conformation in solution. This well-defined conformation represents the culmination of the evolutionary design of these biological catalysts, either to create recognition sites for adducts or to force reactants into appropriate transition states favoring particular reaction pathways.^{1,2} The detailed structure that exists for a native protein is a result of two independent processes. The most fundamental process involves the internal search for a global minimum in the free energy.¹⁻³ The other process involves the formation of metastable forms of the protein such as those due to the constraints involved during its synthesis on the ribosome. Some of these metastable forms may be locked in by disulfide bond formation, which then locks in the tertiary structure.^{1,2} The tertiary structure may also be locked in if the energy barrier to the global energy minimum is too high such that the protein cannot energetically search the conformational subspace containing the energy minimum.

The overall, or tertiary, structure of a protein is based on locally ordered secondary structural forms of the chain backbone, such as α -helix, β -sheet, β -turn, and random coil forms. These secondary structures are determined primarily by local interactions and are constrained by the low-energy conformations of the peptide linkages. Extensive experimental and theoretical studies¹⁻³ indicate that peptide secondary structures are based on the planar *trans* peptide group. This is the result of the intrinsically lower energy of the *trans* compared to the *cis* peptide form, estimated to be 2.3-2.6 kcal/mole for *N*-methylacetamide (NMA),⁴⁻⁶ and the high energy associated with unfavorable side-chain interactions for some adjacent peptide units, estimated to favor the *trans* peptide by 10³-fold.³ Nevertheless, non-proline residue *cis* peptides are found experimentally in NMA by NMR,^{5,7} in bombolitin by NMR,^{8a} and in carboxypeptidase by X-ray crystallography.^{8b} In view of the recent claim for the observation of *cis* peptides by UV resonance Raman spectroscopy,⁹ and because this claim involves the reassignment of a new amide band that we recently discovered,¹⁰⁻¹² we have reexamined the vibrational spectrum and structure of

NMA and a series of small peptides.

Recent studies of UV resonance Raman spectra of polypeptides and proteins have led to the characterization of the relationships between their secondary structures and the intensities and frequencies of resonance-enhanced bands associated with the peptide linkage.¹⁰⁻¹⁴ These results demonstrate that the amide II, amide III, and amide II' bands are uniquely enhanced by the ca. 190-nm amide $\pi-\pi^*$ electronic transition,¹⁰⁻¹⁷ while the amide I band derives its intensity from the ca. 160-nm amide $n-\sigma^*$ electronic transition.¹² More recently, we reported the UV resonance enhancement of a uniquely conformation sensitive vibrational mode of peptides and proteins with excitation into the peptide $\pi-\pi^*$ electronic transition.¹⁰⁻¹² This band, which is found between ca. 1300 and 1450 cm^{-1} in peptides, is due to the overtone of the amide V vibration (2 \times amide V), a fundamental mode that involves primarily C-N torsion plus N-H out-of-plane bend.¹⁸ The en-

(1) Cantor, C. R.; Schimmel, P. R. *Biophysical Chemistry Part I. Conformation of Biological Macromolecules*; Freeman: San Francisco, 1980.

(2) Stryer, L. *Biochemistry*, 2nd ed.; Freeman: San Francisco, 1981.

(3) Creighton, T. E. *Proteins; Structure and Molecular Properties*; Freeman: New York, 1983; pp 159-197.

(4) Ataka, S.; Takeuchi, H.; Tasumi, M. *J. Mol. Struct.* **1984**, *113*, 147-160.

(5) Radzicka, A.; Pedersen, L.; Wolfenden, R. *Biochemistry* **1988**, *27*, 4538-4541.

(6) Jorgensen, W. L.; Gao, J. *J. Am. Chem. Soc.* **1988**, *110*, 4212-4216.

(7) Barker, R. H.; Boudreaux, G. J. *Spectrochim. Acta A* **1967**, *23A*, 727-728.

(8) (a) Bairaktari, E.; Mierke, D. F.; Mammi, S.; Peggion, E. *J. Am. Chem. Soc.* **1990**, *112*, 5383. (b) Rees, D. C.; Lewis, M.; Honzatko, R. B.; Lipscomb, W. N.; Hardman, K. D. *Proc. Natl. Acad. Sci. U.S.A.* **1981**, *78*, 3408-3412.

(9) Wang, Y.; Purrello, R.; Spiro, T. G. *J. Am. Chem. Soc.* **1989**, *111*, 8274-8276.

(10) Song, S.; Asher, S. A.; Krimm, S.; Bandekar, J. *J. Am. Chem. Soc.* **1988**, *110*, 8547-8548.

(11) Krimm, S.; Song, S.; Asher, S. A. *J. Am. Chem. Soc.* **1989**, *111*, 4290-4294.

(12) Song, S.; Asher, S. A. *J. Am. Chem. Soc.* **1989**, *111*, 4295-4305.

(13) Copeland, R. A.; Spiro, T. G. *Biochemistry* **1987**, *26*, 2134-2139.

(14) Copeland, R. A.; Spiro, T. G. *J. Am. Chem. Soc.* **1986**, *108*, 1281-1285.

(15) Dudik, J. M.; Johnson, C. R.; Asher, S. A. *J. Phys. Chem.* **1985**, *89*, 3805-3814.

(16) Mayne, L. C.; Ziegler, L. D.; Hudson, B. J. *J. Phys. Chem.* **1985**, *89*, 3395-3398.

(17) Mayne, L. C.; Hudson, B. *Proceedings of the 11th International Conference on Raman Spectroscopy*; Clark, R. J. H., Long, D. A., Eds.; Wiley: Chichester, U.K., 1988; pp 745-746.

* Author to whom correspondence should be addressed.

[†] University of Pittsburgh.

[‡] University of Michigan.

hancement of this overtone derives from the twisted ca. 190-nm amide $\pi-\pi^*$ excited state; the torsional component of the mode distorts the ground-state geometry toward that of the excited state. The frequency of $2 \times$ amide V was found to be very sensitive to the polypeptide backbone conformation,¹⁰⁻¹² a consequence of the strong dependence of the fundamental (through its N-H out-of-plane bend component) on the peptide hydrogen-bond strengths in different conformations. We proposed that a similar assignment applied to the enhanced 1496-cm⁻¹ band of aqueous NMA, particularly in view of the amide V fundamental frequency found near 750 cm⁻¹.¹⁰ Recently, Wang et al.⁹ suggested that high 200-nm laser excitation fluxes photoisomerize *trans*-NMA to the *cis* form. Since such high fluxes lead to intensity increases in the band at 1496 cm⁻¹, they concluded that this band should be assigned to amide II of *cis*-NMA and that the NMA band at ca. 1380 cm⁻¹ (labeled "amide S") was a better candidate for the overtone assignment.

These assignments are crucial for understanding amide ground-state geometries and amide photochemistry and for determining the geometry of the amide excited state. Further, the band in question offers unique promise as a marker of protein and peptide secondary structure. For all of these reasons it is essential to understand the precise origin of this band. We have therefore carefully examined the NMA photochemistry and the temperature dependence of enhanced bands in NMA and small model peptides to characterize the origin of the 1496-cm⁻¹ band in NMA and the peptide *trans*-*cis* isomerization. We also have obtained resonance Raman spectra of isotopically substituted NMA, glycylglycine (DGL), and *N*-acetylglycine (AGL) as well as resonance Raman spectra of solid-state DGL to confirm the assignments of bands in these molecules. We have measured UV absorption and resonance Raman spectra of model compounds of *cis* peptides and tertiary amides to characterize the enhancement mechanisms of *cis* peptide vibrations and to compare these with modes of *trans* peptides. We conclude that our original assignment¹⁰⁻¹² of the $2 \times$ amide V band in peptides, polypeptides, and proteins is correct but that the 1496-cm⁻¹ band in NMA is indeed assignable to amide II of *cis*-NMA.⁹ However, the assignment⁹ of the ca. 1380-cm⁻¹ band of NMA to an overtone of amide V is incorrect. Our studies indicate that previous analyses of the vibrational dynamics of *cis*-amides need modification. Finally our studies confirm the conclusion that the $\pi-\pi^*$ excited state of the peptide group is twisted.

Experimental Section

N-Methylacetamide (NMA), 2-acetidinone (AZE), 2-pyrrolidinone (PYR), δ -valerolactam (VAL), ϵ -caprolactam (CAP), *N,N*-dimethylacetamide (DMA), and sodium perchlorate were obtained in the highest purity available from Aldrich Chemical Co. 2,5-Piperazinedione (diketopiperazine, DKP), glycylglycine (DGL), glycylglycine amide (DGLA), glycylglycylglycine (TGL), *N*-acetylglycine (AGL), L-analyl-L-alanine (DLA), L-valyl-L-valine (DLV), and α -L-glutamyl- α -L-glutamic acid (DLG) were purchased from Sigma Chemical Co. *N*-*tert*-Butylacetamide (NBA) was purchased from Schweizerhall and *N*-(hydroxymethyl)acetamide (NHMA) from Alfa Chemical Co. All samples were used without further purification, except for NBA which was recrystallized before use. [¹³C]Glycyl[¹⁵N]glycine (¹³C¹⁵N-DGL) was synthesized according to the method described in our previous paper.¹¹ *N*-Methylacet-*d*₃-amide (C-*d*₃-NMA) was obtained by adding acetyl-*d*₃ chloride (Aldrich, 99% isotopic purity) to an excess of methyllamine which was trapped at dry ice temperature in a pressure bottle. *N*-Acetyl-*d*₃-glycine (C-*d*₃-AGL) was prepared by adding acetic-*d*₆ anhydride (Aldrich, 99% isotopic purity) to glycine in methanol with 2 equiv of NaOH at 0 °C. After the pH was adjusted to 3 with sulfuric acid, solid C-*d*₃-AGL was obtained and recrystallized in methanol. The identity and purity of the final isotopic products were confirmed by proton NMR and mass analysis.

The UV resonance Raman spectrometer, which is described in detail elsewhere,¹⁹ utilized a Nd:YAG system operated at 20 Hz with pulse widths of ca. 4 ns. UV radiation was generated by mixing the doubled dye output with the 1.06- μ m YAG fundamental. The Raman scattered

light was collected in a 135° backscattering geometry. NMA samples were irradiated in a single pass by using a 1 mm i.d. Suprasil capillary with a flow rate of ca. 8 cm/s. For high pulse energy we used a windowless sampling system where the sample was pumped through a dye-laser jet nozzle by a magnetic gear pump at a flow rate of ca. 400 cm/s. The sample thickness is estimated to be ca. 200 μ m at 1 mm from the nozzle tip. Other samples (ca. 10–25 mL) in solution state were recirculated through a 1 mm i.d. Suprasil quartz capillary by a peristaltic pump. The flow rate was sufficient to supply fresh sample to the irradiated sample volume between laser pulses. Raman spectra of static, nonflowing samples were obtained by using a 1 mm i.d. Suprasil capillary. The pulse energies were attenuated either by changing the laser spot size by translating the 25 cm focal length lens prior to the sample or by placing Suprasil neutral density filters in the beam path. The spot size of the beam was measured by translating a razor blade mounted on a micrometer stage across the beam and monitoring the power using a Scientech Model 361 power meter.²⁰ NMA sample concentrations were typically 100 mM with 1 M NaClO₄ as an internal intensity standard. This gave an absorption of 0.8 for the capillary and 0.16 for the jet sample thickness. Raman cross sections were derived from measured peak height ratios between Raman bands of analytes and those of the internal standard by using our previously measured Raman cross sections of the 932-cm⁻¹ band of NaClO₄.²¹ We experimentally verified that our laser excitation conditions caused inconsequential sample heating for the flowing samples (vide infra). Resonance Raman spectra of solid DGL were obtained from a NaCl pressed pellet containing ca. 10% of DGL by weight. The resulting 1.3-cm pellets were rotated in the sample beam, and the sample was changed after each 1-min scan. The scattered light was collected in a 135° backscattering geometry. Ordinary Raman spectra were obtained on a Spex 1403 spectrometer with Ar⁺ 514.5-nm excitation and ca. 500-mW power. Infrared spectra were obtained on a Bomem DA-3 FTIR spectrometer with a circle cell having a ZnSe crystal or on a Mattson Cygnus 100 FTIR spectrometer with AgCl windows with a ca. 5- μ m spacer. Solid-state IR spectra were obtained from sodium chloride pellets.

We searched for any permanent photochemistry for the NMA samples from the high pulsed laser power by measuring 300-MHz proton NMR spectra as well as Raman spectra of intensely irradiated samples. In the NMR experiment, 1 mL of 100 mM NMA in D₂O was irradiated by 220-nm light with ca. 1200 mJ/(cm² pulse) for 1.5 h (2500 photons/molecule). No additional peaks were observed. In the Raman experiment, an NMA sample in H₂O was irradiated with ca. 1200 mJ/(cm² pulse) for 1 h (170 photons/molecule), and then the spectrum was obtained at a lower level of 4.4 mJ/(cm² pulse). No change was observed compared to the spectrum obtained from a fresh sample examined at this lower power flux.

The UV absorption spectra were measured with a Perkin-Elmer Model Lambda 9 UV-vis-NIR spectrophotometer installed with a far-UV N₂ purge assembly. All Raman and absorption spectra were measured at room temperature, unless otherwise specified; the accuracy of temperatures listed below is ± 0.5 °C for absorption measurements and ± 3 °C for Raman measurements.

Results

***N*-Methylacetamide.** Figure 1 shows representative resonance Raman spectra of aqueous NMA excited at 220 nm as a function of pulse energy flux. Figure 1A was obtained by tight focusing of the laser beam on the sample, resulting in an energy flux of ca. 1160 mJ/(cm² pulse). Figure 1E shows the lowest power flux spectrum [4.4 mJ/(cm² pulse)] obtainable with a high signal-to-noise ratio. The 932-cm⁻¹ band is the symmetric stretching vibration of ClO₄⁻ used as an internal intensity standard. The dominant bands at 1581 and 1316 cm⁻¹ are the amide II and III modes, respectively, of *trans*-NMA, which derive from vibrations involving C-N stretching and N-H in-plane bending.^{10,11,14-16,18} These bands are selectively enhanced by the amide $\pi-\pi^*$ electronic transition due to the C-N bond elongation in the excited state.¹⁰⁻¹⁷ The 1382-cm⁻¹ band has previously been assigned to the symmetric bend of the (C)CH₃ group,^{11,15,22} although this assignment has recently been questioned by Wang et al.⁹ (vide infra). The 1496-cm⁻¹ band, which we previously assigned to the overtone of

(20) Teraoka, J.; Harmon, P. A.; Asher, S. A. *J. Am. Chem. Soc.* **1990**, *112*, 2892-2900.

(21) Dudik, J. M.; Johnson, C. R.; Asher, S. A. *J. Chem. Phys.* **1985**, *82*, 1732-1740.

(22) Sugawara, Y.; Hirakawa, A. Y.; Tsuboi, M. *J. Mol. Spectrosc.* **1984**, *108*, 206-214.

(18) Krimm, S.; Bandekar, J. *Adv. Protein Chem.* **1986**, *38*, 181-364.

(19) Asher, S. A.; Johnson, C. R.; Murtaugh, J. J. *Rev. Sci. Instrum.* **1983**, *54*, 1657-1662.

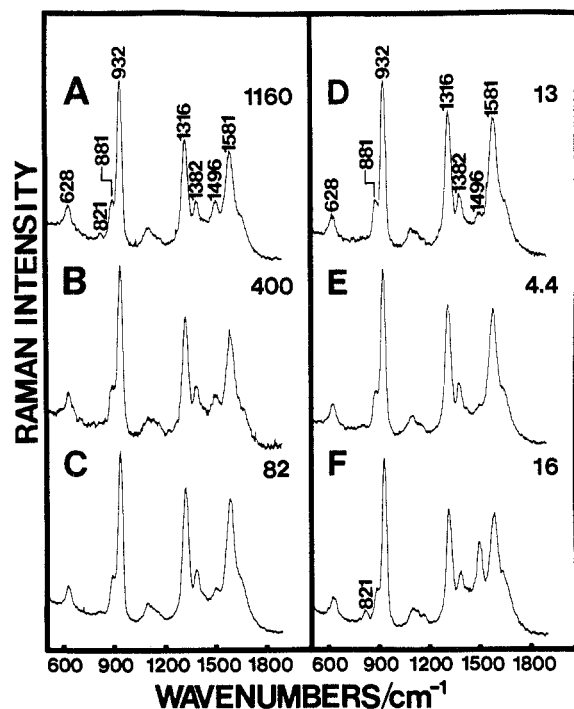


Figure 1. Resonance Raman spectra excited at 220 nm of flowing samples of 0.1 M NMA in water at different pulse energy flux values (A-E). Spectrum F is of a nonflowing sample. The pulse energy flux values listed are in mJ/(cm² pulse). The 932-cm⁻¹ band is from 1 M NaClO₄ used as an internal intensity standard. The spectra were normalized to maintain the ClO₄⁻ peak height identical to permit direct comparison of the amide band intensities.

amide V,^{10,11} has recently been assigned by Wang et al.⁹ to the amide II mode of photoinduced *cis*-NMA. Although we clearly observe this band even at the lowest pulse energy flux of 4.4 mJ/cm² pulse (Figure 1E), we now agree with the Wang et al. assignment of this band to the *cis* form of NMA (vide infra). In addition, a new band at 821 cm⁻¹ appears with an excitation energy flux of ca. 1160 mJ/(cm² pulse). The 881-cm⁻¹ band of *trans*-NMA is expected to shift down by ~60 cm⁻¹ for the *cis* form.^{4,23} Figure 1F shows the UV resonance Raman spectrum of a non-flowing NMA sample in which the 1496-cm⁻¹ band becomes very intense and the 821-cm⁻¹ band becomes prominent. These results also indicate that the 821-cm⁻¹ band is due to *cis*-NMA.

The intensities of the amide II and III bands as well as the internal intensity standard band increase linearly with an increasing pulse energy flux density. Within experimental error we observe no alterations in the intensities of the *trans*-amide bands relative to the perchlorate band up to 1160 mJ/(cm² pulse), the maximum pulse energy flux examined. Figure 2 shows the energy flux dependence of the relative intensity increase of the 1496-cm⁻¹ band compared to that of the ClO₄⁻ band. The 1496-cm⁻¹-band intensity increases nonlinearly, which is consistent with the Wang et al.⁹ observation that this band is photochemically induced. We see less photochemistry with 220-nm excitation than do Wang et al.⁹ with 200-nm excitation because the NMA molar absorptivity at 220 nm (80 M⁻¹ cm⁻¹) is 40-fold less than that at 200 nm (3300 M⁻¹ cm⁻¹) and because the pulse energy fluxes used in our experiment²⁴ are substantially below those of Wang et al.⁹ Our 4.4 mJ/(cm² pulse) low-power flux conditions result in <10⁻⁴ photons absorbed/NMA molecule in the illuminated sample volume, while the 1160 mJ/cm² pulse energy flux results in the absorption of 0.35 photons/NMA molecule. The existence of the 1496-cm⁻¹ band even at low excitation pulse energy fluxes clearly indicates that this band *also* derives from an equilibrium NMA species.

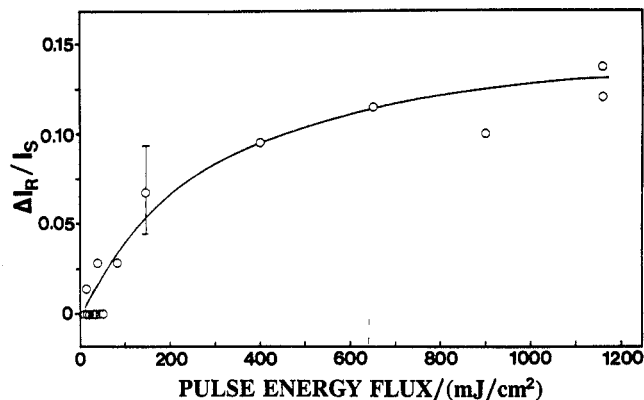


Figure 2. Dependence of the ratio of the increased 1496-cm⁻¹-band intensity (compared to that at the lowest power flux) relative to the intensity of the 932-cm⁻¹ ClO₄⁻ band as a function of pulse energy flux (220-nm excitation).

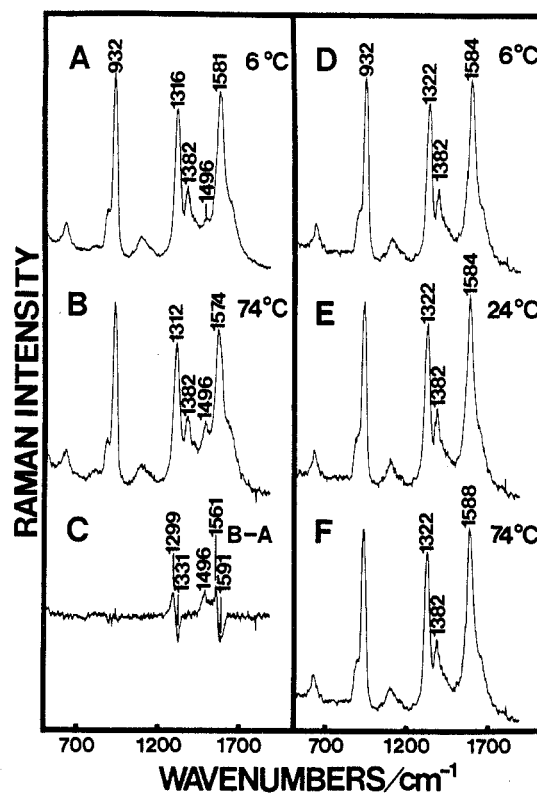


Figure 3. Resonance Raman spectra of 0.1 M NMA at (A) 5 and (B) 74 °C and (C) their difference spectrum, and reconstructed Raman spectra of pure *trans*-NMA (D) at 6, (E) 24, and (F) 74 °C (excitation at 220 nm). Energy flux used is ca. 4.8 mJ/(cm² pulse). The Raman spectra were normalized to obtain identical intensities of the internal intensity standard (peak height). See text for details.

To distinguish photochemically induced *trans*-*cis* isomerization from a thermally induced isomerization, which could result from a temperature increase of the irradiated sample by the excitation beam, Raman spectra of NMA were measured in the presence and absence of sodium nitrate as an absorbing species at identical power fluxes. Since any temperature increase depends simply on the number of photons absorbed by NO₃⁻ per unit volume, a change in absorbance is directly related to a temperature change in the illuminated sample volume. By alteration of the sodium nitrate concentration, the absorbances of NMA samples could be varied from 0.16 to 2.32 across the 0.2-mm jet-nozzle thickness. Neither intensity changes nor any amide band frequency shifts were observed at these pulse energy fluxes. Thus, we conclude that the intensity increase of the 1496-cm⁻¹ band derives solely from photoisomerization of NMA.

(23) Mirkin, N. G.; Krimm, S. Unpublished results.

(24) An energy flux of 10 mJ/(cm² pulse) in this paper corresponds to 1.7 MW/(cm² pulse) in ref 9.

Figure 3 illustrates the resonance Raman spectra of NMA between 500 and 1900 cm^{-1} at various temperatures. Parts A and B of Figure 3 show spectra excited at 220 nm with ca. 4.8 $\text{mJ}/(\text{cm}^2 \text{ pulse})$ at 6 and 74 $^{\circ}\text{C}$, respectively. The intensity of the 1496- cm^{-1} band increases with increasing temperature without any apparent frequency shift, while the *trans*-amide II and amide III bands shift down by 7 and 4 cm^{-1} , respectively. The same frequency shifts of the amide II and III bands are seen in the infrared spectra (not shown). Such shifts could be due to a weakened N-H...O hydrogen bonding at elevated temperatures, which would lower the frequency of the N-H in-plane bending component and thus lower the frequencies of the amide II and III modes. The difference spectrum between the two temperatures (Figure 3C) clearly shows the increase in the 1496- cm^{-1} -band intensity. The accompanying decreases in the amide II and III band intensities of *trans*-NMA are small and difficult to discern. We observe a more dramatic intensity increase in the 1496- cm^{-1} band in Raman spectra of nonflowing samples of NMA at a pulse energy of ca. 16 mJ/cm^2 (Figure 1F): the intensity of this band in this case becomes comparable to that of the amide II band, while the amide II and III band intensities decrease slightly. In this case the repetitive excitation pulses into the nonreplenished illuminated sample volume must result in a large steady-state temperature rise.

Recent theoretical^{5,6} and NMR studies^{5,7} of NMA indicate that *trans*-NMA has a lower enthalpy by ca. 2.5 kcal/mol than *cis*-NMA in aqueous solution. Since the entropies are essentially identical for the *cis* and *trans* forms, the free energy difference is ca. 2.5 kcal/mol. This energy difference indicates that the *cis* isomer should be present to the extent of 1.1%, 1.5% and 2.7% at 6, 24, and 74 $^{\circ}\text{C}$, respectively, from a simple Boltzmann distribution. If we assume that the difference spectrum in Figure 3C reflects the increased concentration of *cis*-NMA (1.6%) between 6 and 74 $^{\circ}\text{C}$ and we subtract the appropriate contribution of the putative *cis* form at each temperature from the Raman spectra obtained at each temperature, we obtain the spectra shown in Figure 3D-F for pure *trans*-NMA at 6, 24, and 74 $^{\circ}\text{C}$, respectively. The bands at 1496 and 821 cm^{-1} are absent, consistent with their assignment to *cis*-NMA, which indicates that the 1496- cm^{-1} band observed in the lower power regime is associated with the equilibrium concentration of this species at ambient temperature.

The existence at 1496 cm^{-1} of a *cis*-amide vibration with a large component of C-N stretching is inconsistent with previous normal mode calculations of isolated *cis*-NMA⁴ and isolated *N*-methylformamide.²⁵ Our previous resonance Raman studies of DKP^{9,10} and Wang et al.'s more recent study of the *cis*-amide caprolactam⁹ as well as the *cis* peptide results here all show a dominant band at ca. 1500 cm^{-1} . This clearly indicates that *cis* peptides have a ca. 1500- cm^{-1} vibration with a large component of C-N stretching, which is required for strong enhancement within the amide π - π^* transition. Experimental²⁶ and normal mode²⁷ studies of DKP lead to similar conclusions. This pattern of enhancement which is localized in only one vibration is reminiscent of the amide II' enhancement for amides in which the N-H is substituted by N-D. For N-D amides the C-N stretching and N-H in-plane bending motions involved in the amide II and III modes become decoupled, and the amide II' vibration is almost a pure C-N stretch. If the 1496- cm^{-1} band of *cis*-NMA is indeed dominated by C-N stretching with a decreased N-H in-plane bending, this would explain its modest frequency dependence upon temperature; changes in hydrogen bonding with temperature are expected to affect primarily the N-H in-plane bend component.

The Raman cross section of the 1496- cm^{-1} putative *cis*-NMA mode appears to be extraordinarily large as determined by its increase in intensity with temperature. We estimate the cross section to be 60 ± 5 mbarns/(mol sr) at 220-nm excitation, a value ca. 10-fold greater than those of the amide II and III bands of

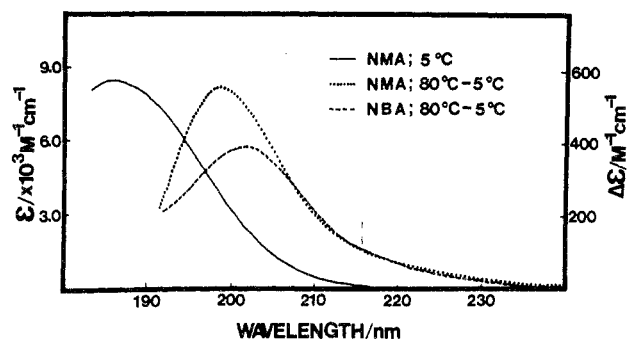


Figure 4. UV absorption spectra of NMA at 5 $^{\circ}\text{C}$ (—) and absorption difference spectra between absorption spectra of NMA (···) and NBA (---) obtained at 80 vs 5 $^{\circ}\text{C}$.

Table I. Absorption and Raman Data for *cis*-Amide II Raman Bands of Lactams and Tertiary Amine^a

molecule ^b	in H ₂ O					in D ₂ O	
	ν^c	σ_{220}^d	λ_{max}^e	ϵ_{max}^f	ϵ_{220}^g	ν^c	σ_{220}^d
AZE	1404	3.4	185.4	6600	90	1375	2.8
PYR	1455	13.2	189.2	7300	160	1443	15.0
VAL	1506	34.5	195.0	7300	360	1497	31.5
CAP	1500	58.2	196.8	7800	710	1493	62.4
DKP	1533 ^h	11.0 ^h	188.0	7000	260	1520 ^h	26.0 ^h
DMA	1509	75.7	195.2	9200	1180	1510	71.5

^a With 220-nm excitation. ^b AZE, 2-azetidinone; PYR, 2-pyrrolidinone; VAL, δ -valerolactam; CAP, ϵ -caprolactam; DKP, 2,5-piperazinedione; DMA, *N,N*-dimethylacetamide. ^c Frequency in cm^{-1} . ^d Cross section in mbarn/(molecule sr). ^e Absorption maximum in nm. ^f Molar absorptivity at maximum in $\text{M}^{-1} \text{cm}^{-1}$. ^g Molar absorptivity at 220 nm in $\text{M}^{-1} \text{cm}^{-1}$. ^h For 218-nm excitation, from ref 12.

trans-NMA, which are ca. 4.7 and 6.3 mbarns/(mol sr), respectively. The present cross-section values for *trans*-NMA are significantly larger than those measured by Dudik et al.,¹⁵ probably because they used high-power fluxes that caused a depletion of the *trans*-NMA species.

This increased Raman cross section of *cis*-NMA derives from a large red shift in its π - π^* transition compared to that in the *trans* peptides. Figure 4 shows the absorption spectrum of NMA at 5 $^{\circ}\text{C}$. The absorption maximum occurs at 186 nm with a molar absorptivity of 8450 $\text{M}^{-1} \text{cm}^{-1}$. With increasing temperature, the intensity of the 186-nm π - π^* electronic transition decreases, while the absorbance at longer wavelengths increases. Figure 4 also shows the NMA difference spectrum between 80 and 5 $^{\circ}\text{C}$, corrected for the specific volume change at 80 $^{\circ}\text{C}$ according to the data of Kell.²⁸ The absorption difference maximum at 198.5 nm must derive from contributions of the *cis*-NMA π - π^* electronic transition and from an increased contribution from hot bands.

We have attempted to deconvolute the hot-band contribution from that of the *cis* peptide by systematically examining the temperature difference spectra for related compounds. The temperature absorption difference spectra of diglycine (DGL), dialanine (DLA), and divaline (DLV) between 80 and 5 $^{\circ}\text{C}$ show broad doublets between 200 and 220 nm. The components of this doublet may separately derive from hot-band absorption and the formation of a *cis* peptide. In contrast, *N-tert*-butylacetamide (NBA) does not appear to form a *cis* peptide even with nonflowing samples with excitation flux condition which would lead to formation of *cis*-NMA, DGL, DLA, and DLV. Thus, the Figure 4 NBA temperature absorption difference spectrum must result solely from an increased "hot-band" contribution. Assuming identical hot-band contributions for NMA and NBA at 80 $^{\circ}\text{C}$, we can estimate a molar absorptivity of $7000 \pm 2000 \text{ M}^{-1} \text{cm}^{-1}$ for *cis*-NMA. This estimated molar absorptivity value is similar to that for the *cis* constrained lactams and for DKP. Table I lists the absorption spectral properties of *cis* peptide model complexes,

(25) Sugawara, Y.; Hirakawa, A. Y.; Tsuboi, M.; Kato, S.; Morokuma, K. *Chem. Phys.* **1981**, *62*, 339-351.

(26) Cheam, T. C.; Krimm, S. *Spectrochim. Acta A* **1984**, *40A*, 481-501.

(27) Cheam, T. C.; Krimm, S. *Spectrochim. Acta A* **1984**, *40A*, 503-517.

(28) Kell, G. S. *J. Chem. Eng. Data* **1967**, *12*, 67-68.

Table II. Raman Bands Assigned to the *cis*- and *trans*-Amide II and II' Bands in Model Peptides^a

molecule ^b	in H ₂ O			in D ₂ O			
	$\nu(c-II)^{c,d}$	$\nu(t-II)^{c,d}$	R^f	$\nu(c-II')^{c,d}$	$\nu(t-II')^{c,d}$	S^g	T^h
NMA	1496	1581	1.057	1480	1504	1.016	1.011
C- <i>d</i> ₃ -NMA	1496	1581	1.057	1476	1504	1.019	1.014
N- <i>d</i> ₃ -NMA ^e	1471	1571	1.067	1471	1497	1.018	1.000
NBA	—	1574	—	—	—	—	—
AGL	1487	1578	1.061	—	—	—	—
C- <i>d</i> ₃ -AGL	1486	1574	1.059	—	—	—	—
DGL	1487	1574	1.059	1463	1499	1.025	1.016
¹³ C ¹⁵ N-DGL	1453	1554	1.070	—	—	—	—
DLA	1483	1567	1.057	—	—	—	—
DLV	1473	1567	1.064	—	—	—	—
DLG	1469	1571	1.069	—	—	—	—
TGL	1487	1574	1.059	—	—	—	—

^a With 220-nm excitation. ^b NMA, *N*-methylacetamide; C-*d*₃-NMA, *N*-methylacet-*d*₃-amide; N-*d*₃-NMA, *N*-methyl-*d*₃-acetamide; NBA, *N*-*tert*-butylacetamide; AGL, *N*-acetylglycine; C-*d*₃-AGL, *N*-acetyl-*d*₃-glycine; DGL, glycylglycine; ¹³C¹⁵N-DGL, [¹³C]glycyl[¹⁵N]glycine; DLA, L-alanyl-L-alanine; DLV, L-valyl-L-valine; DLG, α-L-glutamyl-α-L-glutamic acid; TGL, glycylglycylglycine. ^c Frequency in cm⁻¹. ^d *c*-II, *cis*-amide II; *t*-II, *trans*-amide II; *c*-II', *cis*-amide II'; *t*-II', *trans*-amide II'. ^e From ref 9. ^f $R = \nu(t-II)/\nu(c-II)$. ^g $S = \nu(t-II')/\nu(c-II')$. ^h $T = \nu(c-II)/\nu(c-II')$.

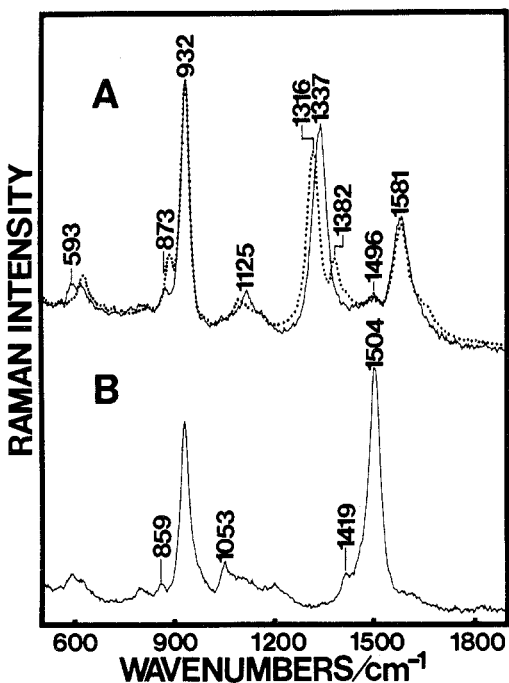


Figure 5. Resonance Raman spectra of (A) 114 mM C-*d*₃-NMA (solid line) and 100 mM NMA (dashed line) in H₂O and (B) 116 mM C-*d*₃-NMA in D₂O. The 932-cm⁻¹ band is that of 1 M NaClO₄. Pulse energy flux is ca. 27 mJ/(cm² pulse), and the spectral resolution is 7 cm⁻¹.

while Table II lists the Raman band frequencies of the complexes discussed in this work. The *cis*-NMA absorption maximum is red-shifted by 12.5 nm compared to that of *trans*-NMA, which may account for the 10-fold increased *cis*-amide Raman cross section for the 1496-cm⁻¹ vibration for 220-nm excitation compared with that of the *trans* peptides. This enhancement permits the easy detection of 1.5% of the *cis* form present at room temperature.

We estimated the quantum yield for formation of the *cis*-NMA. For excitation with 1160 mJ/(cm² pulse), the intensities of the *trans*-NMA bands decrease very slightly, while that of the 1496-cm⁻¹ *cis* band increases. The magnitude of the increase suggests an average concentration of *cis*-NMA of ca. 3.1% of that in the *trans* form. Since this pulse energy flux corresponds to ca. 0.35 photons/molecule absorbed in the illuminated sample volume, we can estimate a lower limit for the quantum yield for *trans*-*cis* photochemical conversion. The ca. 1.6% increase in the equilibrium *cis* form represents a weighted average over the 4-ns laser pulse. Thus, the total increase over the excitation pulse is ca. 3.2%, which would give a quantum yield for formation of the *cis* form of ca. 0.09. This estimate is a lower limit because it neglects any *cis* to *trans* conversion in the ground state.

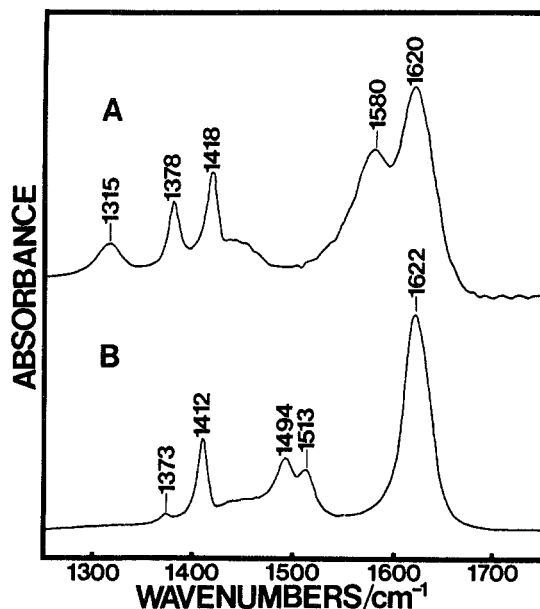


Figure 6. Infrared spectra of (A) 1.6 M NMA in H₂O and (B) ca. 1.6 M NMA in D₂O.

Figure 5 compares the 220 nm excited resonance Raman spectrum of C-*d*₃-NMA in water and in D₂O with that of NMA. Compared to NMA in H₂O, the amide III band shifts by ca. 20 cm⁻¹ to higher frequency while the frequencies of the amide II band and the band at 1496 cm⁻¹ remain unchanged. The most dramatic change in the spectrum is the disappearance of the 1382-cm⁻¹ band of NMA and the appearance of bands at 1125 cm⁻¹ in H₂O and at 1053 cm⁻¹ in D₂O. (The 1504-cm⁻¹ band in D₂O is the amide II' band.)

A band previously observed at ca. 1380 cm⁻¹ in NMA, which is very strong in infrared spectra^{10,29,30} and in visible wavelength Raman spectra, has been previously assigned to the symmetric bend of (C)CH₃^{22,29}; its deuteration shifts, both C-*d*₃ and ND, are also consistent with this assignment.^{22,29} However, Wang et al.⁹ recently reassigned this band to an amide mode on the basis of its disappearance on N-deuteration of *N*-methyl-*d*₃-acetamide (N-*d*₃-NMA). This is not a sufficient argument since the situation is very complex. It has been known that, for neat NMA, the relative intensity of the ca. 1380-cm⁻¹ band in the infrared spectrum decreases significantly on N-deuteration.²⁹ We have found the same to be true for aqueous NMA (see Figure 6). The reason for this is probably the change in the nature of the normal mode on N-deuteration,²² from an eigenvector that contains some

(29) Schneider, B.; Horeni, A.; Pivcova, H.; Honzl, J. *Collect Czech. Chem. Commun.* **1965**, *30*, 2196-2213.

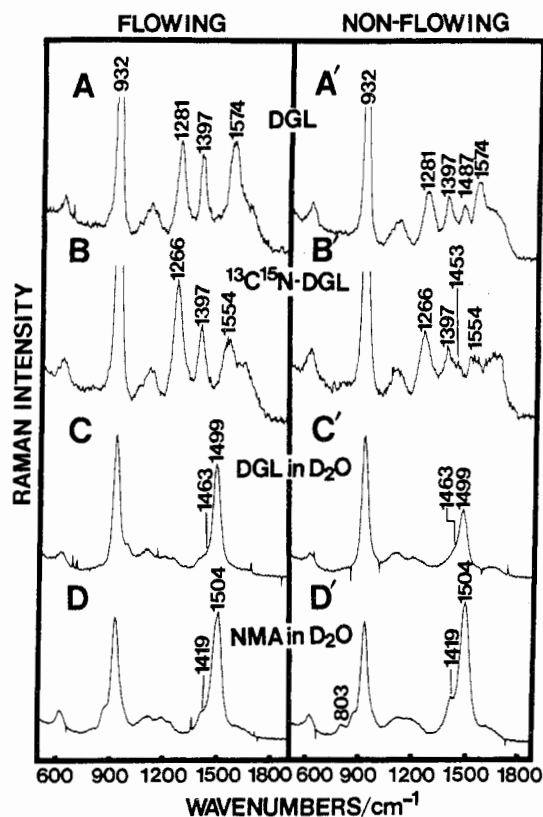


Figure 7. Resonance Raman spectra obtained for flowing and nonflowing samples of (A) 22.9 mM DGL in water, (B) 22.3 mM $^{13}\text{C}^{15}\text{N}$ -DGL in water, (C) 22.9 mM DGL in D_2O , and (D) 102 mM NMA in D_2O . The intensities of the Raman bands of the flowing and nonflowing samples were normalized to each other and to the intensity of ClO_4^- . The pulse energy fluxes used are between 7 and 70 mJ/cm^2 .

C–C(H_3) stretch to one that is almost pure (C)CH $_3$ symmetric bend. Therefore, resonance Raman enhancement of this band is expected to change on N-deuteration. In addition, the assignment of the 1382- cm^{-1} band to an amide V overtone by Wang et al.⁹ can be rejected on the basis of its lack of solvent dependence. The amide V frequency of *trans*-NMA varies tremendously in the condensed phase as a function of "solvent": 619 cm^{-1} in a N_2 matrix,⁴ 660 cm^{-1} in acetonitrile,³¹ 725 cm^{-1} for neat NMA,³⁰ ca. 743 cm^{-1} in water,¹⁰ and 780 cm^{-1} in the crystal.³² However, the frequency of the ca. 1380- cm^{-1} band shows no frequency dependence as a function of acetonitrile–water concentration.¹⁷ This result, as well as our studies on C- d_3 -NMA, shows that the ca. 1380- cm^{-1} band of NMA cannot be assigned to an amide V overtone mode and that it derives from a mode involving mainly (C)CH $_3$ symmetric bending.

Glycylglycine and Analogues. Parts A, B, and C of Figure 7 show the spectra of DGL in H_2O , $^{13}\text{C}^{15}\text{N}$ -DGL in H_2O , and DGL in D_2O , respectively, with 220-nm excitation. The spectra in Figure 7A', B', and C' were obtained under similar conditions but without flowing the sample. The amide II and III bands of DGL occur at 1574 and 1281 cm^{-1} , respectively.^{11,12} The 20- cm^{-1} downshift of amide II and the 15- cm^{-1} downshift of amide III on $^{13}\text{C}^{15}\text{N}$ isotopic substitution occur because of the large C–N stretch component in these modes. The 1397- cm^{-1} band in the DGL spectrum does not shift on isotopic substitution, consistent with its assignment to 2 \times amide V.^{11,12} It should be noted that this 1397- cm^{-1} band is unrelated to the strong bands seen near this position in DGL crystals,^{33,34} which dominate the ordinary Raman

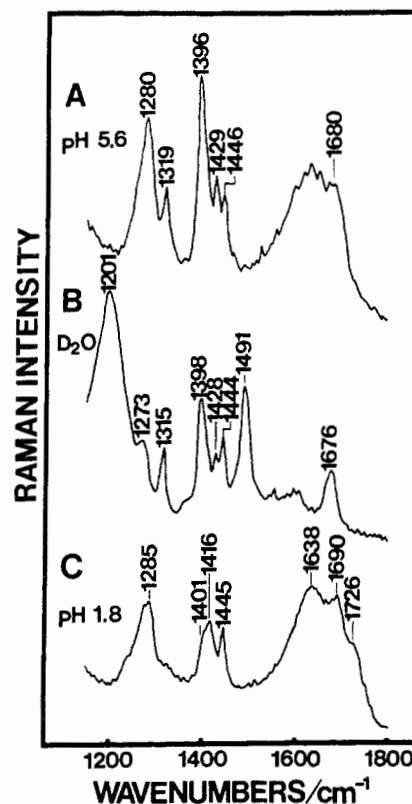


Figure 8. Raman spectra (514.5-nm excitation) of (A) 0.5 M DGL in H_2O at pH 5.6, (B) 0.5 M DGL in D_2O , and (C) 0.5 M DGL in H_2O at pH 1.8.

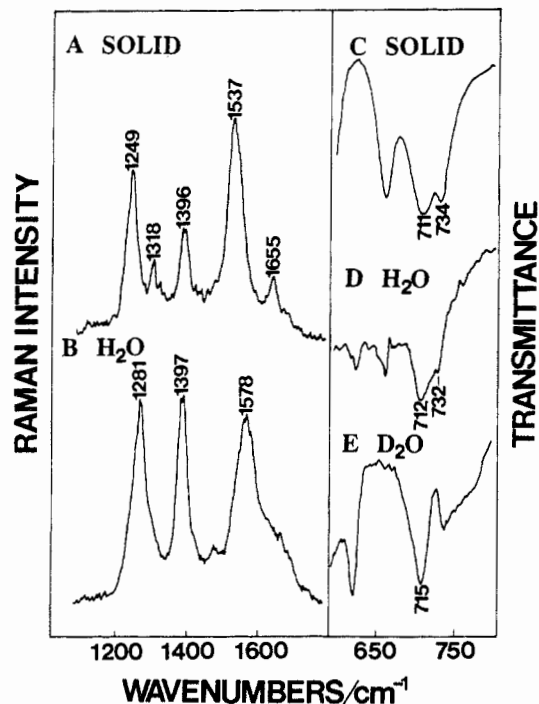


Figure 9. Resonance Raman spectra of (A) 10% solid DGL in a NaCl pellet and (B) 23 mM DGL in water excited at 220 nm and IR spectra of (C) 10% solid DGL in a NaCl pellet, (D) saturated DGL in water at pH 8.6, and (E) saturated DGL in D_2O at pH 8.6.

spectra (as well as infrared absorption spectra) of aqueous solutions of DGL (see Figure 8). The band at 1396 cm^{-1} observed in Raman spectra excited in the visible spectral region does not disappear on N-deuteration but does disappear at low pH, where

(30) Miyazawa, T.; Shimanouchi, T.; Mizushima, S. *J. Chem. Phys.* **1956**, *24*, 408–418.

(31) Fillaux, F.; Baron, M. H. *Chem. Phys.* **1981**, *62*, 275–285.

(32) Dellepiane, G.; Abbate, S.; Bose, P.; Zerbi, G. *J. Chem. Phys.* **1980**, *73*, 1040–1047.

(33) Destrade, C.; Dupart, E.; Jousset-Dubien, M.; Garrigou-Lagrange, C. *Can. J. Chem.* **1974**, *52*, 2590–2602.

(34) Lagant, P.; Vergoten, G.; Loucheux-Lefebvre, M. H.; Fleury, G. *Biopolymers* **1983**, *22*, 1267–1283.

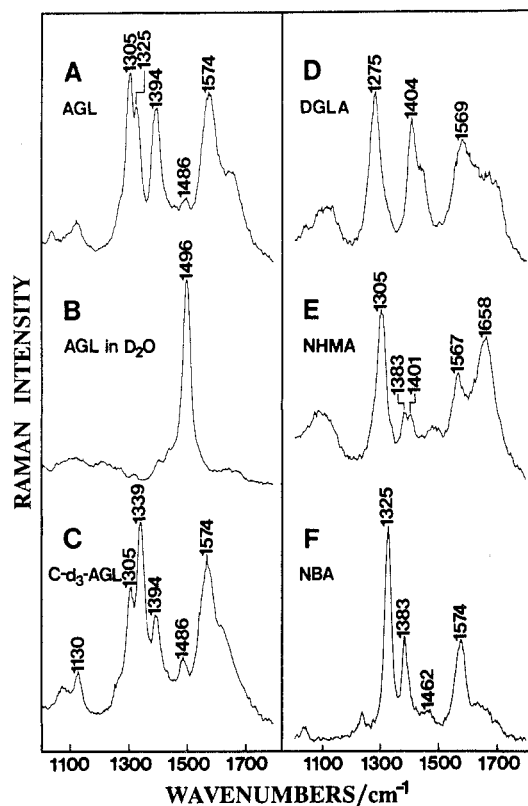


Figure 10. Resonance Raman spectra of (A) 33.8 mM AGL in water and (B) in D_2O , (C) 33.9 mM $C-d_3$ -AGL, (D) 30.0 mM DGLA, (E) 33.7 mM NHMA, and (F) 0.1 M NBA in water. All samples were at pH 7.0. Excitation wavelength is 220 nm. Resolution is 14 cm^{-1} .

COO^- is converted to $COOH$. In contrast, in the UV Raman spectra the 1397-cm^{-1} band disappears upon N-deuteration^{11,12} and remains prominent even at low pH.¹² Thus, this 1397-cm^{-1} band observed with visible excitation derives from the COO^- symmetric stretch. This emphasizes the point¹⁰⁻¹² that the assignment of a resonance-enhanced Raman band does not necessarily coincide with that of a band observed at a similar frequency with nonresonance Raman excitation.

Our assignment of the 1397-cm^{-1} band to $2 \times$ amide V is strongly supported by a comparison between UV resonance Raman spectra and IR spectra of DGL in the solid state and in water. Figure 9 shows Raman spectra of DGL in the solid state and in water with 220-nm excitation. Compared to aqueous DGL, the solid-state DGL amide II and III bands shift down by ca. 30 cm^{-1} , while the 1397-cm^{-1} band barely shifts to 1396 cm^{-1} . The frequency shifts observed for the amide II and III bands are consistent with those observed in a previous nonresonance Raman study.³³ Figure 9 also shows IR spectra of DGL in the solid state, in water and in D_2O . The solid-state 711- and 734-cm^{-1} bands derive from the amide V and the COO^- bending vibrations, respectively.^{11,33-35} In aqueous solution the ca. 712-cm^{-1} band can be assigned to amide V because it disappears in D_2O . The shoulder at 732 cm^{-1} in water and the 715-cm^{-1} band in D_2O derive from COO^- bending.³³⁻³⁵ The fact that the frequency of the 1396 (1397)- cm^{-1} band is somewhat less than twice the amide V fundamental frequency of ca. 711 (712) cm^{-1} in the solid state (or aqueous solution) is indicative of anharmonicity found for these types of vibrations.¹¹ The modest IR frequency change which occurs for the amide V fundamental between the solid state and aqueous solution is essentially identical with the small UV Raman frequency shift present between the solid state and aqueous solution.

Figure 10 shows the 220 nm excited resonance Raman spectra of *N*-acetylglycine (AGL) in water and in D_2O , *N*-acetyl- d_3 -glycine ($C-d_3$ -AGL), glycylglycine amide (DGLA), *N*-(hydroxymethyl)acetamide (NHMA), and NBA in water. As we dis-

cussed previously for AGL,¹² the 1574- and the 1305-cm^{-1} bands are the amide II and III modes which occur at higher frequency than for other peptides because of contributions of CH_3 deformation.³⁶ Interestingly, an additional band is observed at 1325 cm^{-1} which was not noted in previous lower resolution spectra.¹² This band may contain some C-N stretching in view of its enhancement. The 1394- and 1486-cm^{-1} bands are from $2 \times$ amide V (in part) and cis peptide vibrations, respectively. The cis peptide band becomes very intense for nonflowing samples in a manner similar to DGL in Figure 7. The resonance Raman spectrum of $C-d_3$ -AGL in Figure 10C is similar to that of AGL, but the amide III band appears to shift ca. 30 cm^{-1} to higher frequency from that of AGL in a similar manner to that for $C-d_3$ -NMA (Figure 5). We do not at present understand the origin of the $1305/1325\text{ cm}^{-1}$ doublet. The intensity of the 1394-cm^{-1} band of $C-d_3$ -AGL is approximately half of that in AGL. A new band appears at 1130 cm^{-1} , which derives from the CD_3 deformation. This shift leads to a decreased intensity for the 1394-cm^{-1} band. The $2 \times$ amide V is no longer overlapped by the CH_3 deformation.

Thus, AGL and $C-d_3$ -AGL show bands at 1394 cm^{-1} that are easily assigned to the $2 \times$ amide V mode. The amide derivative of diglycine, DGLA (Figure 10D), and the methyl ester¹¹ also show a Raman spectra similar to DGL (Figure 7A) with a strong ca. 1400-cm^{-1} band which is assigned to $2 \times$ amide V. In contrast, the ca. 1400-cm^{-1} $2 \times$ amide V band is not evident for NMA or for other derivatives that do not contain a carbonyl group adjacent to the amide linkage. As indicated in Figure 10E,F, no mode easily assignable to $2 \times$ amide V occurs for either NHMA or NBA. This result suggests an important role for the enhancement of the $2 \times$ amide V band by carbonyl functional groups adjacent to the amide linkage (vide infra).

In the nonflowing DGL sample an additional band occurs at 1487 cm^{-1} , while the intensities of the amide II and III and 1397-cm^{-1} bands decrease (Figure 7). We also observed this band at the same frequency in a flowing sample excited with an energy flux of ca. $1200\text{ mJ}/(\text{cm}^2\text{ pulse})$ (spectrum not shown). On $^{13}C^{15}N$ isotopic substitution, the 1487-cm^{-1} band shifts to 1453 cm^{-1} , showing that it has a large C-N stretching component. In fact, its C-N stretch component is larger than that of amide II of *trans*-NMA: its $^{13}C^{15}N$ isotopic shift ratio ($1487/1453$) is 1.023 compared to $1574/1554 = 1.013$ for *trans*-amide II (a pure C-N stretch would have a ratio of 1.038). It is interesting to note that the $^{13}C^{15}N$ isotopic shift ratio for the N-deuterated *trans*-amide II' band of DGL in D_2O , viz., $1499/1458 = 1.028$ (cf. parts C and D of Figure 1 of ref 11), is close to the shift ratio for the putative *cis*-amide II 1487-cm^{-1} band in DGL. This indicates, as suggested above, that the so-called *cis*-amide II mode has a relatively small contribution from N-H in-plane bending and thus does not shift much on N-deuteration.

We have looked carefully for the *cis*-amide II' mode in both NMA (Figure 7D,D') and $C-d_3$ -NMA (Figure 5), as well as in DGL in D_2O solution (Figures 7C,C'). Difference spectra between the flowing and nonflowing samples show bands at 1480 and 1419 cm^{-1} in NMA, at 1476 and 1419 cm^{-1} in $C-d_3$ -NMA, and at 1463 cm^{-1} in DGL. The 1419-cm^{-1} band observed for NMA and $C-d_3$ -NMA is not a likely candidate, since its frequency shift on deuteration ($1496/1419 = 1.054$) is too large. This enhanced 1419-cm^{-1} band can be assigned to the (N) CH_3 symmetric bend, since this mode acquires a C-N stretching component on N-deuteration.²² (This is consistent with the absence of this band in the high photon flux Raman spectra of $N-d_3$ -NMA in water and D_2O .) We therefore agree with Wang et al. that the 1471-cm^{-1} band of $N-d_3$ -NMA and by analogy the 1480-cm^{-1} band of NMA and the 1476-cm^{-1} band of $C-d_3$ -NMA, as well as the 1463-cm^{-1} band of DGL, are assignable to the amide II' band of the *cis* peptide conformers. The NH/ND frequency shift ratios, $1496/1480 = 1.011$ for NMA, $1496/1476 = 1.014$ for $C-d_3$ -NMA, $1471/1471 = 1.00$ for $N-d_3$ -NMA,⁹ and $1487/1463 = 1.016$ for DGL, are significantly less than that for *trans*-amide

(35) Sundius, T.; Krimm, S. Unpublished results.

(36) Sankaranarayanan, V. N.; Krishnan, P. S. *Indian J. Pure. Appl. Phys.* **1972**, *10*, 378-381.

II', 1581/1504 = 1.051, reflecting the significantly smaller N-H in-plane bending contribution for the *cis*-amide II band. [The fact that the *trans*-amide II'/*cis*-amide II' ratios for NMA in D₂O (1.016) and C-*d*₃-NMA in D₂O (1.019) (see Table II), as well as N-*d*₃-NMA in D₂O⁹ (1.018), are so similar to the *trans*-amide II/*cis*-amide II ratio of NMA isolated in a N₂ matrix⁴ (1.018) also indicates that N-H in-plane bend is much reduced in the *cis*-amide II mode.] Table II also lists the putative *cis*-amide II bands of model compounds that we studied. All of these compounds show a dominant *cis* peptide band between 1469 and 1487 cm⁻¹.

Lactams and Tertiary Amides. Since cyclic lactams are constrained to be *cis*-amides, they should be good models to examine the vibrational and electronic transitions of the *cis*-amide geometry. Wang et al.⁹ previously examined CAP; we report here on a larger series including AZE, PYR, and VAL, as well as DKP and the tertiary amide DMA. Table I lists the amide II and II' frequencies as well as the λ_{\max} values and molar absorptivities of the π - π^* transitions.

For AZE, a band is observed at 1385 cm⁻¹ in the solid that is assigned to a C-N stretch plus N-H in-plane bend by normal mode analysis.³⁷ It is likely that the strong band that we see in this region at 1404 cm⁻¹ in aqueous solution is assignable to this mode, the frequency difference being due to the difference in environment. The 29-cm⁻¹ downshift in D₂O suggests an N-H in-plane bend component to the mode. For PYR, a band is observed in the neat liquid at 1495 cm⁻¹ that is mostly C-N stretching by normal mode analysis.³⁸ The 1455-cm⁻¹ band observed in aqueous solution presumably derives from this mode. This band downshifts by 12 cm⁻¹ in D₂O, although there is an apparent ca. 5-cm⁻¹ increase in the case of the neat compound.³⁸ For VAL, a band at 1497 cm⁻¹ is assigned to CH₂ bend.³⁹ However, this assignment is inconsistent with its observed 6-cm⁻¹ downshift on N-deuteration and with strong enhancement in resonance Raman spectra. For DKP, a very detailed normal mode analysis²⁷ shows that the 1533-cm⁻¹ band is a mode containing C-N stretching plus N-H in-plane bending, and for DMA a similar analysis⁴⁰ shows that the 1509-cm⁻¹ band is a mode with C-N stretching plus (N)CH₃ antisymmetric bending (its lack of shift in D₂O of course follows from the absence of N-H in the molecule). These results also strongly support the assignment of *cis*-amide II in unstrained lactams to a band near 1500 cm⁻¹, thus strengthening the basis for assigning the comparable band in the photoinduced NMA and peptides to this mode. The small shifts on N-deuteration are also consistent with this assignment. The cross sections of lactam compounds and the tertiary amide in water are similar to those in D₂O. This fact suggests a similar contribution of C-N stretching in the *cis*-amide II mode. It is interesting that the absorption maxima of the unstrained lactams are red-shifted by ca. 10 nm from that of *trans*-NMA, in a manner clearly similar to that of the absorption spectrum of the thermally populated *cis*-NMA species. This also supports its assignment to *cis*-NMA. Since the molar absorptivities are similar to that of NMA, we conclude that this red shift is responsible for the increased 220-nm *cis*-NMA Raman cross section over that of the *trans* peptides.

Discussion

The results presented above make a convincing case that the 1496-cm⁻¹ band enhanced by high-energy pulses or elevated temperatures in aqueous NMA should be assigned to the *cis*-amide II mode, as suggested by Wang et al.⁹ (We use the term *cis*-amide II by analogy with the presence of the C-N stretch component, even though the N-H in-plane bend component is much smaller.) Its cross section is ca. 60 mbarns/(mol sr). We have also shown

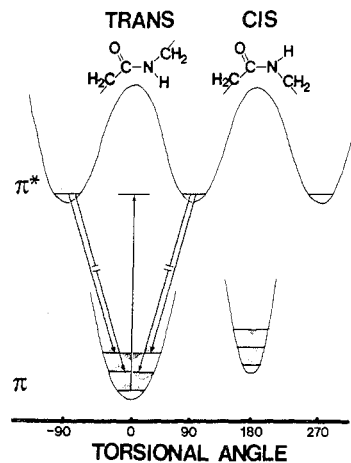


Figure 11. Schematic potential energy diagram of amide *cis* and *trans* ground-state and π^* excited-state manifolds in the amide V coordinate.

that the 821-cm⁻¹ band of NMA is associated with *cis*-NMA. Our studies further demonstrate that a variety of small peptides can be converted from the *trans* to the *cis* peptide by photoisomerization with high-energy UV pulses, the presence of the *cis* structure being manifested by the appearance of a band in the ca. 1470–1500-cm⁻¹ region. The present work also supports our previous assignment^{10–12} of a band in the 1300–1450-cm⁻¹ region of peptides to 2 \times amide V and proves that the band at 1382 cm⁻¹ in NMA is not assignable to 2 \times amide V, despite the suggestion by Wang et al.⁹

The enhancement of *cis*-amide II derives from its large C-N stretching component, which is also predicted by recent ab initio calculations.²³ This is similar to the case for bands of DKP^{11,12} at 1533 and 806 cm⁻¹, both of which involve ring stretching^{26,27} and for which the preresonant state is at ca. 190 nm, where we observe an absorption maximum (see Table I) that corresponds to the amide π - π^* electronic transition.^{41,42} The intensity of the 1533-cm⁻¹ band dominates the spectrum, and its frequency decreases by 13 cm⁻¹ on N-deuteration,¹² in agreement with prediction.²⁷ The newly observed band at 821 cm⁻¹ in NMA at extremely high pulse energy flux also contains C-N stretching²³ and thus corresponds to the ring stretching mode of DKP at 806 cm⁻¹, whose ca. 20-cm⁻¹ downshift on N-deuteration is also well predicted.²⁷ We always observe a band near 800 cm⁻¹ in all *cis* peptide model compounds, which additionally supports the assignment of the 821-cm⁻¹ band of NMA to a *cis* peptide vibration.

Our assignment of the ca. 1400 cm⁻¹ 2 \times amide V is based on the spectra and normal mode calculations of poly(L-glutamic acid), their α -helix, β -sheet, and random coil conformations,^{10–12} isotopic substitution studies of DGL and its analogues,¹¹ determinations of the preresonance-state frequency,^{11,12} and the pH dependence studies of Raman intensity of model complexes.¹² We observe a strong band near 1400 cm⁻¹ for all dipeptides, tripeptides, and polypeptides (with or without side chains). This makes an alternative assignment of this band to an out-of-plane C-H bending⁴³ unlikely; the spectra of DGL, DLA, and DLV are very similar.

These results raise the question of why the 2 \times amide V band is only enhanced for amide linkages containing a carbonyl group situated one carbon unit away from the amide N-H group. This unique enhancement suggests that the amide π - π^* excited state is significantly perturbed by the presence of the adjacent carbonyl group and that the π^* excited states of peptides differ from those of compounds with isolated amide linkages, such as NMA. These results are provocative in that they may indicate a delocalized conjugate network in the π^* state which could result from hyperconjugation. This delocalization of the amide π network in one of the frontier excited states would have important implications

(37) Hanai, K.; Maki, Y.; Kuwae, A. *Bull. Chem. Soc. Jpn.* **1985**, *58*, 1367–1375.

(38) McDermott, D. P. *J. Phys. Chem.* **1986**, *90*, 2569–2574.

(39) Rey-Lafon, M.; Forel, M. T.; Garrigou-Lagrange, C. *Spectrochim. Acta A* **1973**, *29A*, 471–486.

(40) Dwivedi, A. M.; Krimm, S.; Mierson, S. *Spectrochim. Acta A* **1989**, *45A*, 271–279.

(41) Robin, M. B. *Higher Excited States of Polyatomic Molecules*; Academic Press: New York, 1975; Vol II, pp 140–146.

(42) Ham, J. S.; Platt, J. R. *J. Chem. Phys.* **1952**, *20*, 335–336.

(43) Spiro, T. G. Personal communication.

for peptide structure, as well as for electron transfer along the peptide backbone in proteins.

The unique UV enhancement of the overtone of the amide V vibration in the small peptides, polypeptides, and proteins can be understood by analogy to the similar enhancement of the overtone of the torsional vibration of ethylene due to its twisted π^* excited state.^{44,45} Figure 11 shows a possible energy level diagram in the torsional coordinate where the excited-state minima are symmetrically displaced by 90° from that of the ground state like that in ethylene. Also included is a schematic diagram of the ground-state potential energy manifold in a torsional coordinate in which the *cis*-amide ground-state potential well in the torsional coordinate is drawn to indicate that it differs somewhat from the *trans*-amide V torsional mode. The energy increase of the *cis* form internal energy over the *trans* form is also displayed in the figure.

The diagram demonstrates that the Raman Franck-Condon factors are zero for the fundamental amide V Raman transition in the *trans* form but that it is nonzero for the overtone. For example, the 0-0 transition from the ground state to the electronic excited state is allowed. In contrast, the downward 0-1 transition from the excited state to the ground state which results in the Raman fundamental is forbidden because of the phasing of the $v = 1$ ground-state vibrational wave function. Since the phasing is symmetric for both the upper state and $v = 2$ of the ground state, the overtone is symmetry allowed.

This diagram also indicates the origin of the facile *trans*-*cis* photoisomerization which would occur if the excited π^* state were twisted by 90° . Absorption of a photon populates the π^* excited state; relaxation back into the ground state would be equally likely to result in a *trans* or *cis* peptide, if the excited state were exactly twisted by 90° compared to the ground state and if the *cis* and *trans* ground-state manifolds are similar. Our results for NMA show that the quantum yield for photochemical *trans*-*cis* isomerization is at least 0.09 and may be higher.

The photochemical data indicate that both NMA and the peptides have twisted excited states, in contrast to their ground states which are known to be planar.¹⁻³ The enhancement of the $2 \times$ amide V only for peptides containing an adjacent carbonyl group indicates that for these derivatives this torsional mode has large overtone Franck-Condon factor. This derives from a twisted π^* state as shown in Figure 11. We observe no enhancement for the amide V fundamental but see enhancement of higher even quanta of the amide V vibration for DGL and $^{13}\text{C}^{15}\text{N}$ -DGL; we see $4 \times$ amide V at ca. 2780 cm^{-1} (slight anharmonicity is evident) in a manner similar but somewhat less than ethylene. The $4 \times$ amide V/ $2 \times$ amide V intensity ratio is 0.23 for ethylene;²⁴ it is 0.05 for DGL and 0.09 for $^{13}\text{C}^{15}\text{N}$ -DGL. This difference may suggest that the excited state is twisted by less than 90° for DGL and other peptides. The excited-state twist for NMA may be even smaller.

We should note that the enhancement of the even amide V torsional overtones does not by itself *prove* that the excited state is twisted. This enhancement could result from a large change in the torsional force constant in the amide π^* excited state. Whether this could result in the observed relative overtone intensities will require extensive calculations. However, the facile *trans*-*cis* photoisomerization data militate for the conclusion that the amide π^* excited state is twisted.

The facile photochemical conversion of the *trans* to the *cis* form of peptides is reminiscent of the similar photochemical conversion of *N*-(methylthio)acetamide (NMTA) from the *trans* to the *cis* form (and the *cis* to the *trans* form) which has been carefully studied by Harada and Tasumi and others.⁴⁶⁻⁴⁸ The energy difference between the *trans* and *cis* ground states of NMTA is close to that for NMA,^{47,48} and the absorption maximum for the *cis* form is at a longer wavelength than that of the *trans* form. The vibrational spectra, however, differ sufficiently that it is difficult to directly relate the NMTA spectral data directly to our NMA Raman data, and we cannot identify an amide V-like mode. By analogy to the facile *trans*-*cis* photoisomerization of NMA, it appears likely that the NMTA excited state is also twisted compared to the ground state.

As noted above, the establishment of an amide II mode for *cis* peptides, in which N-H bending is a small component of a vibration that is mostly a C-N stretch, is in conflict with the results of a previous normal mode study⁴ which calculated *cis*-amide II and III modes similar to those of the *trans* form. This normal mode calculation is probably in error due to the assumption that the geometry and force constants for the *cis* form could be transferred without change from the *trans* calculation. Recent ab initio calculations show that this is clearly not the case.²³

Conclusions

Photochemical conversion of *trans* peptides into *cis* peptides occurs with a high quantum yield (greater than 0.09) for 220-nm excitation into the *trans* peptide π - π^* transition. The *cis* peptide is easily studied since its Raman cross section is 10-fold larger than that of the *trans* peptide with 220-nm excitation. We can detect the ca. 1.5% Boltzmann population of the *cis* form of NMA at room temperature. The vibrational mode of *cis* peptides differ dramatically from those of *trans* peptides. For example, the *cis*-amide II vibration contains much less N-H in-plane bending than that of the *trans* form. This result is inconsistent with previous normal mode calculations which assumed that the geometry and force constants were the same for the *cis* and *trans* forms. The π^* excited state of peptides is twisted relative to the ground state in a manner reminiscent of ethylene. We also reinterpret the previous data of Harada and Tasumi⁴⁶⁻⁴⁸ to indicate that the π^* state of *N*-(methylthio)acetamide is twisted. Our data clearly indicate the correctness of the assignment of the peptide conformation sensitive band at ca. 1400 cm^{-1} to the overtone of the amide V vibration.¹⁰⁻¹²

Acknowledgment. This research was supported by NIH Grant 1R01GM30741-08 (S.A.A.) and by NSF Grants DMB-8816756 and DMR-8806975 (S.K.). We thank Mr. Sung-Mo Choi and Dr. Wonghil Chang for technical help in synthesizing C-*d*₃-NMA and C-*d*₃-AGL and Prof. Bruce Hudson for helpful discussions.

Registry No. NMA, 79-16-3; C-*d*₃-NMA, 3669-69-0; NBA, 762-84-5; AGL, 543-24-8; C-*d*₃-AGL, 18427-56-0; DGL, 556-50-3; $^{13}\text{C}^{15}\text{N}$ -DGL, 88815-60-5; DLA, 1948-31-8; DLV, 3918-94-3; DLG, 3929-61-1; TGL, 556-33-2; NHMA, 625-51-4; DGLA, 20238-94-2; AZE, 930-21-2; PYR, 616-45-5; VAL, 675-20-7; CAP, 105-60-2; DKP, 106-57-0; DMA, 127-19-5.

(46) Harada, I.; Tasumi, M. *Chem. Phys. Lett.* **1980**, *70*, 279-282.

(47) Kato, C.; Hamaguchi, H.; Tasumi, M. *J. Phys. Chem.* **1985**, *89*, 407-410.

(48) Ataka, S.; Takeuchi, H.; Harada, I.; Tasumi, M. *J. Phys. Chem.* **1984**, *88*, 449-451.

(44) Ziegler, L. D.; Hudson, B. *J. Chem. Phys.* **1983**, *79*, 1197-1202.

(45) Sension, R. J.; Hudson, B. *J. Chem. Phys.* **1989**, *90*, 1377-1389.